

Cultured cambial meristematic cells as a source of plant natural products

Eun-Kyong Lee^{1,5}, Young-Woo Jin^{1,5}, Joong Hyun Park¹, Young Mi Yoo¹, Sun Mi Hong¹, Rabia Amir², Zejun Yan², Eunjung Kwon^{2,3}, Alistair Elfick³, Simon Tomlinson⁴, Florian Halbritter⁴, Thomas Waibel², Byung-Wook Yun² & Gary J Loake²

A plethora of important, chemically diverse natural products are derived from plants¹. In principle, plant cell culture offers an attractive option for producing many of these compounds^{2,3}. However, it is often not commercially viable because of difficulties associated with culturing dedifferentiated plant cells (DDCs) on an industrial scale³. To bypass the dedifferentiation step, we isolated and cultured innately undifferentiated cambial meristematic cells (CMCs). Using a combination of deep sequencing technologies, we identified marker genes and transcriptional programs consistent with a stem cell identity. This notion was further supported by the morphology of CMCs, their hypersensitivity to γ -irradiation and radiomimetic drugs and their ability to differentiate at high frequency. Suspension culture of CMCs derived from *Taxus cuspidata*, the source of the key anticancer drug, paclitaxel (Taxol)^{2,3}, circumvented obstacles routinely associated with the commercial growth of DDCs. These cells may provide a cost-effective and environmentally friendly platform for sustainable production of a variety of important plant natural products.

Only plant stem cells, embedded in meristems located at the tips of shoots and roots or contained inside the vascular system, can divide and give rise to cells that ultimately undergo differentiation while simultaneously giving rise to new stem cells⁴. These cells can be considered immortal due to their ability to theoretically divide an unlimited number of times. Consequently, since the beginnings of tissue culture in the 1940s, cell suspension cultures have been routinely generated through what was believed to be a dedifferentiation process⁵. Recent evidence suggests this mechanism might not entail a simple reverse reprogramming⁶. Regardless of the mechanism involved, this process results in mitotic reactivation of specialized cell types within a given organ, generating a multicellular mixture of proliferating cells⁷. Suspension cultures derived from such cellular assortments often exhibit poor growth properties with low and inconsistent yields of natural products³, owing to deleterious genetic and epigenetic changes that occur during this process^{7,8}.

To circumvent this so-called dedifferentiation procedure, we developed an innately undifferentiated cell line derived from cambium cells, which function as vascular stem cells⁹. Also, paclitaxel biosynthesis in *T. cuspidata* is most conspicuous within the region containing these CMCs¹⁰. A recently developed twig was collected from a wild yew, *T. cuspidata* (Fig. 1a). We gently peeled tissue that contained cambium, phloem, cortex and epidermis from the xylem (Fig. 1b and Supplementary Fig. 1a–c) and confirmed the absence of xylem cells by staining with phloroglucinol-HCl, which detects lignin deposition (Supplementary Fig. 2a–f). After this tissue was cultured on solid isolation medium for 30 d (Fig. 1c), actively proliferating cambium cells could be gently separated from the DDCs derived from phloem, cortex and epidermis (Fig. 1c–e and Supplementary Fig. 3a–e). This mass of proliferating cells was distinct from DDCs derived from a needle or embryo (Fig. 1f,g), and the morphology of these CMCs differed from adjacent cells (Fig. 1h and Supplementary Fig. 3b–e). We also used this technology to produce such cells from a variety of plant species, including ginseng (*Panax ginseng*), ginkgo (*Ginkgo biloba*) and tomato (*Solanum lycopersicon*). This suggests that the procedure has broad utility (Supplementary Fig. 4a–f).

Microscopic analysis of a suspension culture of *T. cuspidata* cells revealed the presence of small, abundant vacuoles within the cultured cells. This characteristic feature of CMCs¹¹ enables them to withstand the pressure generated by the expanding secondary xylem¹². In contrast, dedifferentiated *T. cuspidata* cells derived from needles or embryos possessed only one large vacuole, typical of such plant cells (Fig. 1i,j). The ability to differentiate into either a tracheary element, the main conductive cell of the xylem, or a phloem element is a defining trait of CMCs^{13,14}. These cultured cells could be conditionally differentiated into a tracheary element at high frequency. In contrast, no tracheary elements were formed from *T. cuspidata* DDCs (Fig. 1k,l). Both animal and plant stem cells are particularly sensitive to cell death triggered by ionizing radiation, to safeguard genome integrity in populations of such cells¹⁵. In a similar fashion, these cultured cells are hypersensitive to γ -irradiation (Fig. 1m) and display increased cell death in response to the radiomimetic drug zeocin¹⁵ (Fig. 1n). In aggregate, our findings, based on a variety of

¹Unhwa Corp., Wooah-Dong, Dukjin-gu, Jeonju, South Korea. ²Institute of Molecular Plant Sciences, School of Biological Sciences, University of Edinburgh, King's Buildings, Edinburgh, UK. ³School of Engineering, University of Edinburgh, King's Buildings, Edinburgh, UK. ⁴Institute for Stem Cell Research, School of Biological Sciences, University of Edinburgh, King's Buildings, Edinburgh, UK. ⁵These authors contributed equally to this work. Correspondence should be addressed to G.J.L. (gloake@ed.ac.uk).

Received 24 August; accepted 27 September; published online 24 October 2010; doi:10.1038/nbt.1693

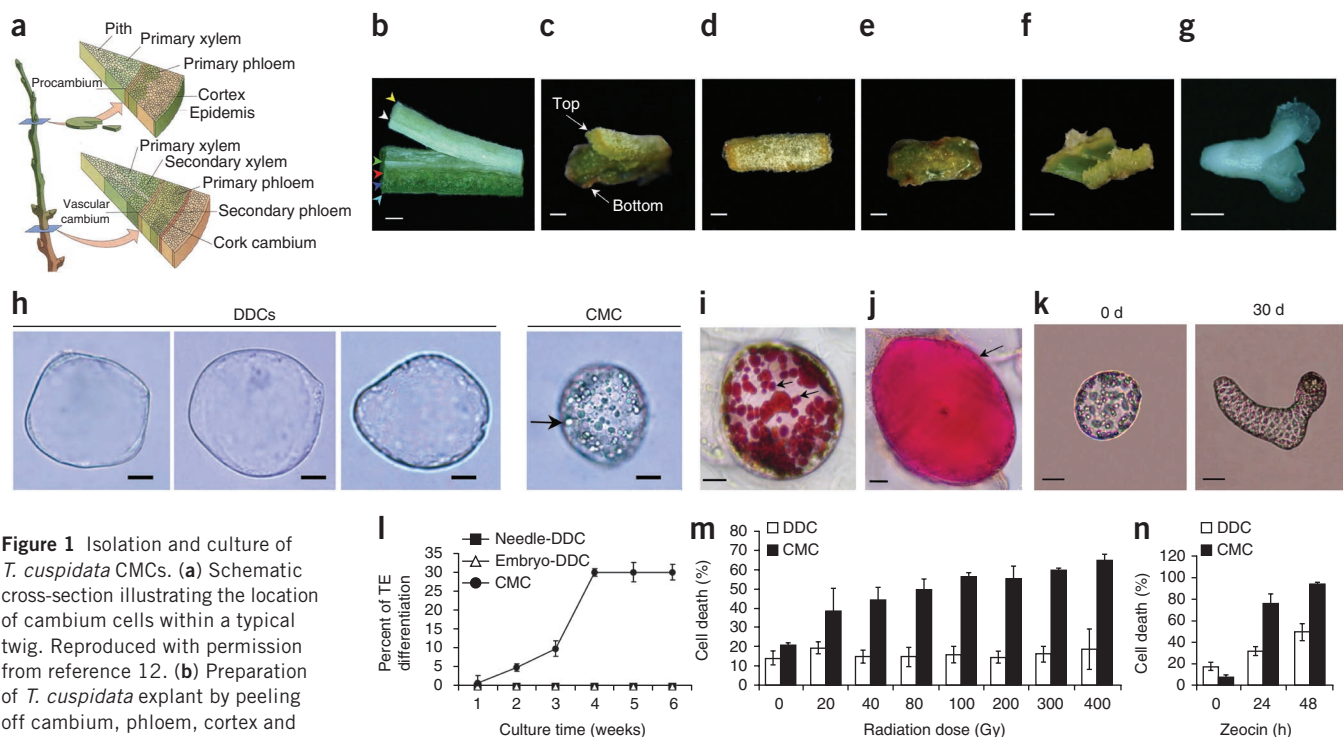


Figure 1 Isolation and culture of *T. cuspidata* CMCs. (a) Schematic cross-section illustrating the location of cambium cells within a typical twig. Reproduced with permission from reference 12. (b) Preparation of *T. cuspidata* explant by peeling off cambium, phloem, cortex and epidermal cells from the xylem. Cell types are indicated by the following colored arrows: yellow, pith; white, xylem; green, cambium; red, phloem; blue, cortex; and turquoise, epidermis. Scale bar, 0.5 mm. (c) Natural split of CMCs from DDCs induced from phloem, cortex and epidermal cells. The top layer is composed of CMCs whereas the bottom layer consists of DDCs. Scale bar, 1 mm. (d) CMCs proliferated from the cambium. Scale bar, 1 mm. (e) DDCs induced from the tissue containing phloem, cortex and epidermal cells. Scale bar, 1 mm. (f) DDCs induced from the cut edge of a needle explant. Scale bar, 0.5 mm. (g) DDCs induced from the cut edge of an embryo explant. Scale bar, 0.5 mm. (h) Micrographs of DDCs and a CMC. CMCs are significantly smaller and possess characteristic numerous, small vacuole-like structures. The black arrow indicates a vacuole-like structure. Scale bars, 20 μ m. (i) Single CMC stained with neutral red, which marks the presence of vacuoles. Two of many stained vacuoles are denoted by black arrows. (j) Needle-derived DDC stained with neutral red. The single large vacuole present in this cell is marked by a black arrow. Scale bar, 10 μ m. (k) Conditional differentiation of *T. cuspidata* CMCs to tracheary elements, at the times indicated, after addition of differentiation media. Scale bar, 25 μ m. (l) Time-course of differentiation of different *T. cuspidata* cell lines over time into tracheary elements. (m) Quantification of cell death in *T. cuspidata* cells after exposure to increasing levels of ionizing radiation. (n) Levels of cell death in *T. cuspidata* cells after exposure to the radiomimetic drug, Zeocin (phleomycin). Experiments were repeated at least twice with similar results. Data points represent the mean of three samples \pm s.d.

approaches, are consistent with the notion that these cultured cells exhibit stem cell-like properties, consistent with a CMC identity.

We used a combination of deep sequencing technologies to compare the molecular signatures of these cells and those of typical DDCs. First, we used an approach based on massively parallel pyrosequencing¹⁶ to profile the *T. cuspidata* transcriptome. A total of 860,800 reads of average length 351 bp generated 301 MB of sequence (Supplementary Fig. 5a and Supplementary Tables 1–3). From these sequence data, we assembled 36,906 contigs *de novo* (average length, 700 bp; maximum length, 10,355 bp), with 8,865 contigs > 1 kb (Supplementary Fig. 5b and Supplementary Tables 4–6). We subjected contigs from the *T. cuspidata* transcriptome (Supplementary Data Set 1) to BLAST searches and 62% were assigned a putative function (Supplementary Data Set 2). This data set should provide an important resource because there is currently no large-scale sequence information derived from this division of the plant kingdom. The determination of the *T. cuspidata* transcriptome enabled us to use digital gene expression tag profiling¹⁶ to compare gene expression in prospective CMCs with gene expression in DDCs (Supplementary Data Set 3) in the absence of exogenous chemical elicitors that can induce paclitaxel biosynthesis.

Digital gene expression tag profiling analysis established that 563 genes were differentially expressed in CMCs, with 296 upregulated and 267 downregulated (Fig. 2a, Supplementary Figs. 6 and 7 and Data Set 4). A subset of these genes were validated by RT-PCR

(Supplementary Fig. 8). *Phloem intercalated with xylem* (*PXY*) encodes a leucine-rich repeat (LRR) receptor-like kinase (RLK), which is conspicuously expressed in CMCs. *PXY* is a member of a small series of closely related LRR RLKs, mutations that impact CMC function¹⁷. *T. cuspidata* contig 01805 exhibits high similarity to *PXY* (Supplementary Fig. 9a) and is differentially expressed in our prospective CMC suspension cells (Supplementary Data Set 4). Analysis by qRT-PCR established that expression of contig 01805 is upregulated ninefold in these cells relative to DDCs (Fig. 2b).

Wooden Leg (*WOL*) encodes a two-component histidine kinase which is a member of a small gene family in *Arabidopsis*¹⁸. *WOL*-like proteins are unique in having two putative receiver or D-domains and mutations in *WOL* affect vascular morphogenesis¹⁸. *WOL* is expressed in the cambium¹⁸ and *WOL*-like genes are expressed in the cambial zone of the silver birch (*Betula pendula*) and poplar (*Populus trichocarpa*)¹⁹. *T. cuspidata* contig 10710 exhibits high similarity to *WOL* and its related genes (Supplementary Fig. 9b). Gene expression analysis established that this gene is upregulated 12-fold in CMCs relative to DDCs (Fig. 2b).

To assess the molecular composition and the relative expression of genes indicative of given biological pathways in our prospective CMCs, we performed enrichment analysis of Gene Ontology (GO) terms within our data set. This approach established that both stress and biotic defense response genes were prominently over-represented

Figure 2 Characterization of CMCs from *T. cuspidata*, including transcriptome profiling using digital gene expression tags. **(a)** Scatter plot showing differentially expressed genes (DEGs) (blue and red) in CMCs and non-DEGs (black). The deployment of further filtering approaches identified more robust DEGs (red), whereas other DEGs (blue) were filtered out. $FDR \leq 0.05$; $n = 1,229$. **(b)** Analysis of the expression of contig 01805 and contig 10710. **(c)** Relative percentage of GO groups within CMC DEGs. **(d)** Growth of CMCs and DDCs derived from needles or embryos on solid growth media from an initial 3 g f.c.w. 95% confidence limits are too small to be visible on this scale. **(e)** Bar graph reporting the extent of cell aggregation in DDC and CMC suspension cultures. **(f)** Paclitaxel production by 3-month-old DDCs and CMCs 10 d after elicitation, following batch culture in a flask format. Error bars represent 95% confidence limits. These experiments were repeated three times with similar results.

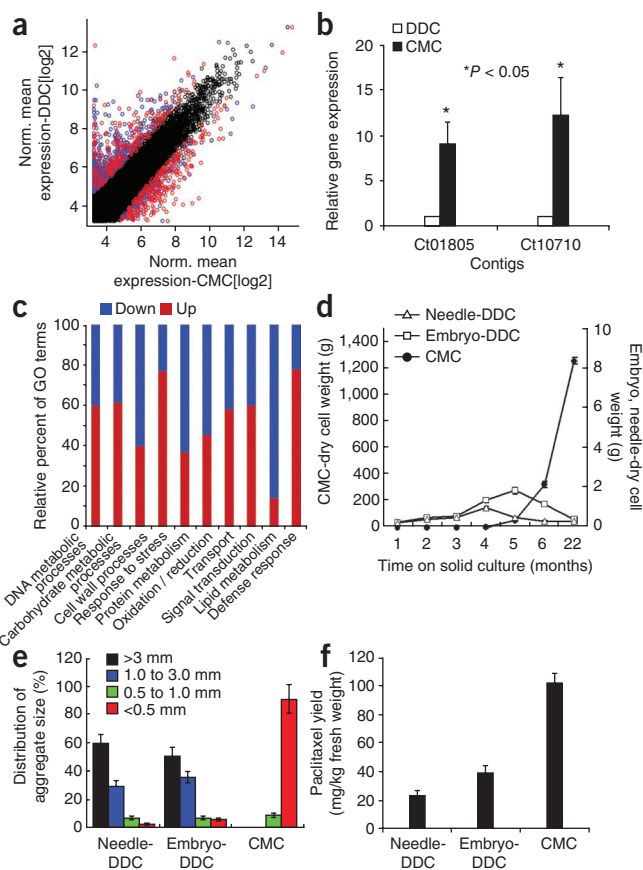
(Fig. 2c). Stem cells exhibit a low threshold for auto-execution through apoptosis but express robust defenses against environmental stresses²⁰. Collectively, our Digital gene expression tag profiling data are therefore consistent with a CMC identity for these cultured cells.

We used a solid growth media format and representative cell lines to compare the growth properties of these CMCs with DDCs derived from the same wild tree. At 22 months after inoculation, the *T. cuspidata* needle- and embryo-derived DDCs produced a total dry cell weight (d.c.w.) of 0.32 g and 0.41 g, respectively, when grown on solid media with subculturing every 2 weeks (Fig. 2d). In contrast, the d.c.w. generated from CMCs was 1,250 g, an increase of $4.0 \times 10^5\%$ and $3.0 \times 10^5\%$, respectively. Moreover, these cells were still growing rapidly following 22 months of culture, whereas DDCs possessed conspicuous necrotic patches (Supplementary Fig. 10) and displayed signs of a rapid decrease in their viable cell biomass.

Pronounced cell aggregation is a typical feature of suspension cultures comprised of DDCs. This can lead to differences in local environments between cells significantly reducing growth rate and natural product biosynthesis³. In representative suspension cultures of DDCs derived from either *T. cuspidata* needles or embryos, the proportion of cell aggregates with a diameter <0.5 mm was only 2% or 5%, respectively ($n = 150$ cells). Conversely, in representative CMCs, 93% of cell aggregates had a diameter <0.5 mm, with many cells present as singletons or components of aggregates comprised of only 2–3 cells ($n = 150$ cells) (Fig. 2e and Supplementary Fig. 11).

We next determined the magnitude of paclitaxel biosynthesis in this novel cell line during batch culture in a 125 ml Erlenmeyer flask. At 14 d after inoculation of flask cultures with cells, cells were transferred to production medium containing the elicitors methyl-jasmonate² and chitosan, together with a precursor phenylalanine, to induce paclitaxel biosynthesis. Levels of paclitaxel were measured 10 d later by high-performance liquid chromatography (HPLC). The amount of paclitaxel produced, 102 mg/kg fresh cell weight (f.c.w.), was conspicuously greater than that generated by either needle or embryo-derived DDCs at a f.c.w. value of 23 mg/kg or 39 mg/kg, respectively (Fig. 2f). Measurements of this natural product were confirmed by liquid chromatography mass spectrometry (LC-MS) (Supplementary Fig. 12a–d). Further, genes encoding key enzymes integral to the biosynthesis of paclitaxel^{2,3} were induced more strongly in CMCs than in DDCs (Supplementary Fig. 13).

To establish whether these cells exhibit superior growth properties on a larger scale, we first investigated their performance in a 10 liter stirred tank bioreactor. In this environment, shear stress can limit growth, and the problem is often intensified by cell aggregation²¹. The CMCs in this bioreactor grew significantly faster than DDCs (Fig. 3a). Further, in response to shear stress, the survival rate of CMCs was strikingly higher than for DDCs, which by the



end of the culture period had largely turned necrotic and had stopped growing (Supplementary Fig. 14a–c).

Next, we explored the performance of these cells in a 3 liter air-lift bioreactor. Large aggregates of DDCs formed in this bioreactor, leading to reduced cell mixing and circulation, which subsequently resulted in cell adherence to the bioreactor wall. Furthermore, many of these adhered cellular aggregates developed necrotic patches. After 4 months of culture, the growth of DDCs from either needle or embryo, expressed as dry cell weight (d.c.w.), were 3.33 g and 5.08 g, respectively. In contrast, the CMC line had generated a d.c.w. of 3,819.44 g, an increase of 114,000% and 75,000%, respectively (Fig. 3b). We also analyzed the growth of these cell lines in a 20 liter air-lift bioreactor, routinely used as a pilot for subsequent large-scale production. DDCs did not grow in this size bioreactor under the conditions tested and rapidly became necrotic. Conversely, CMCs always grew rapidly, increasing their d.c.w. from 3.65 g/l to 12.85 g/l within 14 d (Fig. 3c). Their relative tolerance of shear stress can likely be attributed to their small and abundant vacuoles, reduced aggregation and thin cell walls²¹.

We attempted to improve the performance of needle- and embryo-derived DDCs by specifically selecting the more rapidly growing cells at each subculture on solid media for a period of 1.8 years. This process improved the growth of needle-, but not embryo-derived, DDCs in a 3 liter air-lift bioreactor. However, the performance of CMCs was still strikingly superior to that of these extensively selected cells with respect to specific growth rate (μ), doubling time (T_d) and growth index (GI) (Supplementary Fig. 15 and Supplementary Table 7). A key trait for the exploitation of plant cells on an industrial scale is the stability of their growth in suspension culture³. We therefore monitored the growth stability of these cells compared to selected

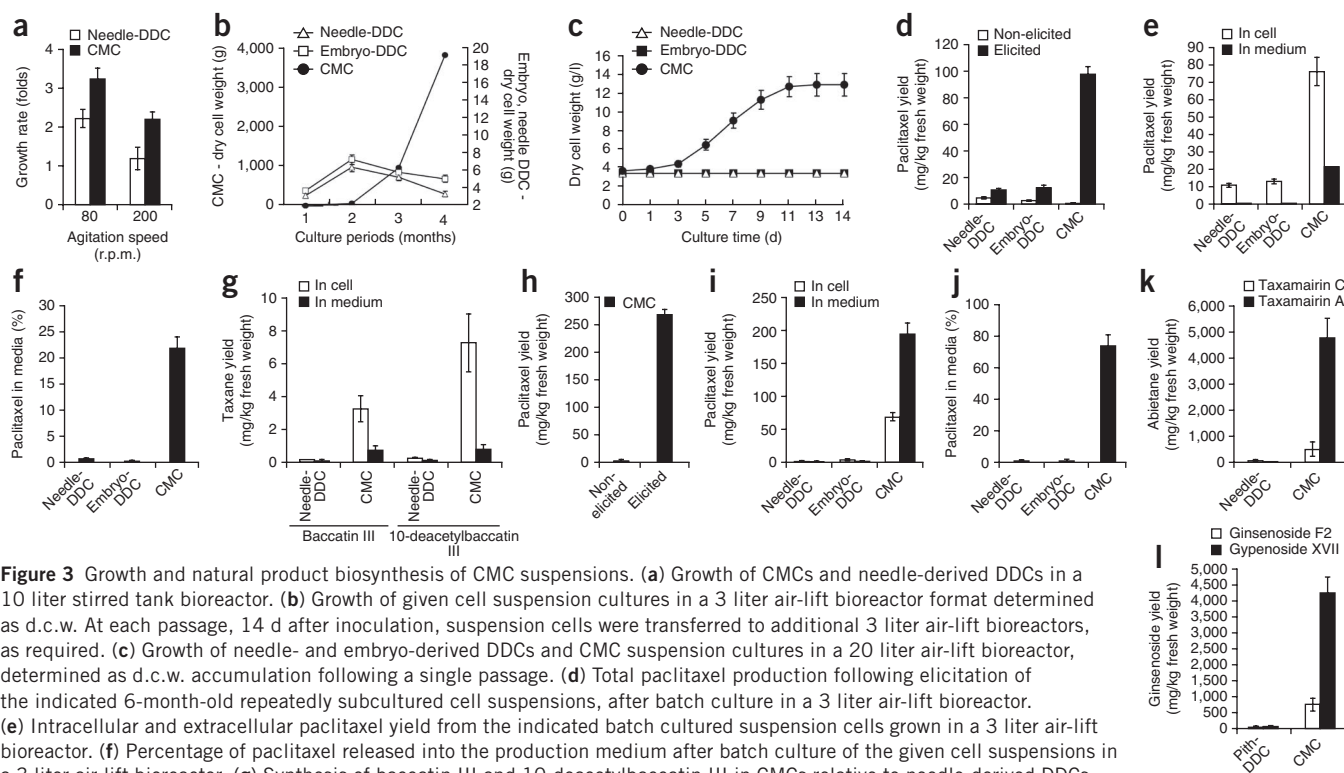


Figure 3 Growth and natural product biosynthesis of CMC suspensions. **(a)** Growth of CMCs and needle-derived DDCs in a 10 liter stirred tank bioreactor. **(b)** Growth of given cell suspension cultures in a 3 liter air-lift bioreactor format determined as d.c.w. At each passage, 14 d after inoculation, suspension cells were transferred to additional 3 liter air-lift bioreactors, as required. **(c)** Growth of needle- and embryo-derived DDCs and CMC suspension cultures in a 20 liter air-lift bioreactor, determined as d.c.w. accumulation following a single passage. **(d)** Total paclitaxel production following elicitation of the indicated 6-month-old repeatedly subcultured cell suspensions, after batch culture in a 3 liter air-lift bioreactor. **(e)** Intracellular and extracellular paclitaxel yield from the indicated batch cultured suspension cells grown in a 3 liter air-lift bioreactor. **(f)** Percentage of paclitaxel released into the production medium after batch culture of the given cell suspensions in a 3 liter air-lift bioreactor. **(g)** Synthesis of baccatin III and 10-deacetylbaaccatin III in CMCs relative to needle-derived DDCs. **(h)** Magnitude of paclitaxel biosynthesis following elicitation of 28-month-old CMCs in a 20 liter air-lift bioreactor. Needle- and embryo-derived DDC suspensions did not routinely grow in this size bioreactor. **(i)** Intracellular and extracellular paclitaxel yield after 45 d of perfusion of cultured needle- and embryo-derived DDCs and CMCs in a 3 liter air-lift bioreactor. **(j)** Percentage of paclitaxel released into the production medium after perfusion culture of the given cell suspensions as indicated in **i**. **(k)** Synthesis of taxamairin A and C in CMCs and needle-derived DDCs after batch culture in a 3 liter air-lift bioreactor. **(l)** Synthesis of ginsenosides in *P. ginseng* CMC and pith-derived DDC suspension cells after batch culture in a 3 liter air-lift bioreactor. Error bars represent 95% confidence limits. These experiments were repeated twice with similar results.

DDCs derived from needles. The CMCs exhibited a relatively constant growth rate over time. In contrast, we observed striking fluctuations in growth rates during the culture of DDCs (**Supplementary Fig. 16**). Finally, we determined the growth of CMCs within a 3 ton bioreactor. These cells were again successfully cultured with high performance (**Supplementary Fig. 17a and b**), establishing their utility for growth on an industrial scale.

We determined the level of paclitaxel production of these different *T. cuspidata* cell suspensions in both 3 liter and 20 liter air-lift bioreactors. At 10 d after elicitation, CMCs again synthesized strikingly more paclitaxel than either of the DDC lines in a 3 liter air-lift bioreactor. Further, elicitation induced a 220% (11 mg/kg) and 433% (13 mg/kg) increase in paclitaxel production within needle- and embryo-derived DDCs respectively, whereas the induction was 14,000% (98 mg/kg) with CMCs (**Fig. 3d**). CMCs secreted $2.7 \times 10^4\%$ and $7.2 \times 10^4\%$ more paclitaxel into the culture medium than the low levels secreted by either needle- or embryo-derived DDCs, respectively (**Fig. 3e,f**). The amount of paclitaxel secreted to the medium during culture varies significantly both between *Taxus* species and in response to different culture conditions²². Our DDCs secreted less paclitaxel than might be expected. Nevertheless, *T. cuspidata* CMCs secreted a strikingly greater amount of paclitaxel into the medium under these culture conditions than the associated DDCs. Moreover, these cells also synthesized strikingly more of the related taxanes baccatin III and 10-deacetylbaaccatin III^{2,3} (**Fig. 3g**). No paclitaxel production was detected by either DDC line in a 20 liter air-lift bioreactor. In contrast, CMCs synthesized 268 mg/kg and were again highly responsive to elicitation (**Fig. 3h**). Previously

reported values for *T. cuspidata* paclitaxel production range from 20–84 mg/kg f.c.w.^{23,24}. However, these data, including the maximum value, were obtained from flask cultures, whereas our data suggest that DDCs have improved function relative to their performance on a larger scale. Our findings imply that CMCs synthesize strikingly more paclitaxel and are significantly more responsive to elicitation when batch cultured in either 3 liter or 20 liter air-lift bioreactors compared to typical *T. cuspidata* suspension cells.

Perfusion culture promotes the secretion of secondary metabolites into the culture medium, aiding both purification and natural product biosynthesis²². We therefore compared the magnitude of paclitaxel secretion after perfusion culture. Following 45 d of perfusion culture, needle- and embryo-derived DDCs were largely necrotic; however, CMCs produced a combined total of 264 mg of paclitaxel per kg of cells and 74% of this was secreted directly into the medium (**Fig. 3i,j**). Perfusion culture of these cells therefore both promotes paclitaxel biosynthesis and increases the proportion of this secondary product that is secreted into the medium, facilitating its cost-effective purification. The future deployment of metabolic engineering approaches and higher yielding *Taxus* species may further enhance paclitaxel biosynthesis in these cells^{2,3}.

We also monitored these *T. cuspidata* suspension cultures for the production of the abietane tricyclic diterpenoid derivatives, taxamairin A and taxamairin C, which have also been shown to possess antitumor activities²⁵. Elicitation of these cells within a 3 liter air-lift bioreactor induced increases in both taxamairin C and especially taxamairin A to 520.8 and 4,982.5 mg/kg f.c.w., respectively, in CMCs. These values were far greater than those determined in

DDCs (Fig. 3k). Suspension cultures of *T. cuspidata* have previously been reported to produce 0.92 and 26.08 mg/kg f.c.w. of taxamairin C and taxamairin A, respectively²⁶. Our data imply that CMCs might provide a considerably better source of these abietanes than DDCs. To establish whether CMCs derived from other plant species also exhibit superior properties with respect to the biosynthesis of commercially relevant natural products, we determined the synthesis of ginsenosides, a class of triterpenoid saponins derived exclusively from the plant genus *Panax*. Ginsenosides have been reported to show multiple bioactivities including neuroprotection, antioxidative effects and the modulation of angiogenesis²⁷. Following elicitation of tap root-derived *P. ginseng* suspension cells, cultured using a 3 liter air-lift bioreactor, ginsenoside F2 and gypenoside XVII accumulated to strikingly greater levels in *P. ginseng* CMCs relative to DDCs. Ginsenoside F2 and gypenoside XVII accrued to 791 and 4,425 mg/kg f.c.w., respectively (Fig. 3l). Previously, ginsenoside F2 has been reported to reach 33.3 mg/kg f.c.w.²⁸ and gypenoside XVII 183.3 mg/kg f.c.w.²⁹ in ginseng roots. Thus, CMCs synthesize 23.8- and 24.1-fold more ginsenoside F2 and gypenoside XVII, respectively, than previously described sources. Therefore, CMCs may also be used for the production of ginsenosides.

Numerous medicines, perfumes, pigments, antimicrobials and insecticides are derived from plant natural products^{1–3,30}. Cultured cambial meristematic cells may provide a cost-effective, environmentally friendly and sustainable source of paclitaxel and potentially other important natural products. Unlike plant cultivation, this approach is not subject to the unpredictability caused by variation in climatic conditions or political instability in certain parts of the world. Furthermore, CMCs from reference species may also provide an important biological tool to explore plant stem cell function.

METHODS

Methods and any associated references are available in the online version of the paper at <http://www.nature.com/naturebiotechnology/>.

Accession codes. Sequence Read Archive: ERP000352.

Note: Supplementary information is available on the Nature Biotechnology website.

ACKNOWLEDGMENTS

T.W. was awarded a BBSRC CASE PhD studentship. This project was funded in part by a grant from the Korea Institute for Advancement of Technology (KIAT) (R & D project number: 10030175), the Ministry of Knowledge Economy (MKE), Republic of Korea to E.-K.L., J.H.P., S.M.H. and G.J.L. R.A. was supported by a scholarship from HEC Pakistan. E.K. was supported by a studentship from the Engineering and Physical Sciences Research Council. We acknowledge the expert technical assistance of A. Montazam and D. Cleven for Roche 454 sequencing and M. Thomson for Illumina Solexa sequencing. Further, S. Bridgett and U. Trivedi provided invaluable input for bioinformatic analysis of the deep sequencing data. All sequencing was undertaken at the GenePool facility, University of Edinburgh.

AUTHOR CONTRIBUTIONS

E.-K.L., Y.-W.J., J.H.P., T.W. and B.-W.Y. performed experiments. R.A., E.K., S.T. and F.H. contributed to bioinformatic and statistical analysis. Z.Y., Y.M.Y. and S.M.H. carried out experiments. A.E. co-supervised E.K. E.-K.L., Y.-W.J. and G.J.L. formulated experiments. G.J.L. and E.-K.L. wrote the paper. All authors discussed results and commented on the manuscript.

COMPETING FINANCIAL INTERESTS

The authors declare competing financial interests: details accompany the full-text HTML version of the paper at <http://www.nature.com/naturebiotechnology/>.

Published online at <http://www.nature.com/naturebiotechnology/>.

Reprints and permissions information is available online at <http://npg.nature.com/reprintsandpermissions/>.

- Schmidt, B.M., Ribnicky, D.M., Lipsky, P.E. & Raskin, I. Revisiting the ancient concept of botanical therapeutics. *Nat. Chem. Biol.* **3**, 360–366 (2007).
- Croteau, R., Ketchum, R.E.B., Long, R.M., Kaspera, R. & Wildung, M.R. Taxol biosynthesis and molecular genetics. *Phytochem. Rev.* **5**, 75–97 (2006).
- Roberts, S.C. Production and engineering of terpenoids in plant cell culture. *Nat. Chem. Biol.* **3**, 387–395 (2007).
- Laux, T. The stem cell concept in plants: a matter of debate. *Cell* **113**, 281–283 (2003).
- Thorpe, T.A. History of plant tissue culture. *Mol. Biotechnol.* **37**, 169–180 (2007).
- Sugimoto, K., Jiao, Y. & Meyerowitz, E.M. *Arabidopsis* regeneration from multiple tissues occurs via a root development pathway. *Dev. Cell* **18**, 463–471 (2010).
- Grafi, G. et al. Histone methylation controls telomerase-independent telomere lengthening in cells undergoing dedifferentiation. *Dev. Biol.* **306**, 838–846 (2007).
- Baebler, S. et al. Establishment of cell suspension cultures of yew (*Taxus x Media* Rehder) and assessment of their genomic stability. *In Vitro Cell. Dev. Biol. Plant* **41**, 338–343 (2005).
- Ye, Z.-H. Vascular tissue differentiation and pattern formation in plants. *Annu. Rev. Plant Biol.* **53**, 183–202 (2002).
- Strobel, G.A. et al. Taxol formation in yew-*Taxus*. *Plant Sci.* **92**, 1–12 (1993).
- Frankenstein, C., Eckstein, D. & Schmitt, U. The onset of cambium activity - A matter of agreement? *Dendrochronologia* **23**, 57–62 (2005).
- Moore, R., Clark, W.D., Stern, K.R. & Vodopich, D. (eds.) *Botany* (Wm.C. Brown, Dubuque, Iowa, USA; 1995).
- Turner, S., Gallois, P. & Brown, D. Tracheary element differentiation. *Annu. Rev. Plant Biol.* **58**, 407–433 (2007).
- Ito, Y. et al. Dodeca-CLE peptides as suppressors of plant stem cell differentiation. *Science* **313**, 842–845 (2006).
- Fulcher, N. & Sablowski, R. Hypersensitivity to DNA damage in plant stem cell niches. *Proc. Natl. Acad. Sci. USA* **106**, 20984–20988 (2009).
- Shendure, J. & Ji, H. Next-generation DNA sequencing. *Nat. Biotechnol.* **26**, 1135–1145 (2008).
- Fisher, K. & Turner, S. PXY, a receptor-like kinase essential for maintaining polarity during plant vascular-tissue development. *Curr. Biol.* **17**, 1061–1066 (2007).
- Mähönen, A.P. et al. A novel two-component hybrid molecule regulates vascular morphogenesis of the *Arabidopsis* root. *Genes Dev.* **14**, 2938–2943 (2000).
- Nieminen, K. et al. Cytokinin signaling regulates cambial development in poplar. *Proc. Natl. Acad. Sci. USA* **105**, 20032–20037 (2008).
- Rando, T.A. The immortal strand hypothesis: segregation and reconstruction. *Cell* **129**, 1239–1243 (2007).
- Joshi, J.B., Elias, C.B. & Patole, M.S. Role of hydrodynamic shear in the cultivation of animal, plant and microbial cells. *Chem. Eng. J.* **62**, 121–141 (1996).
- Wang, C., Wu, J. & Mei, X. Enhanced taxol production and release in *Taxus chinensis* cell suspension cultures with selected organic solvents and sucrose feeding. *Biotechnol. Prog.* **17**, 89–94 (2001).
- Mirjalili, N. & Linden, J.C. Methyl jasmonate induced production of Taxol in suspension cultures of *Taxus cuspidata*: Ethylene interaction and induction models. *Biotechnol. Prog.* **12**, 110–118 (1996).
- Wu, Z.L., Yuan, Y.-J., Ma, Z.-H. & Hu, Z.D. Kinetics of two-liquid-phase *Taxus cuspidata* cell culture for production of Taxol. *Biochem. Eng. J.* **5**, 137–142 (2000).
- Yang, S.-J., Fang, J.-M. & Cheng, Y.-S. Lignans, flavonoids and phenolic derivatives from *Taxus mairei*. *J. Chinese Chem. Soc.* **46**, 811–818 (1999).
- Bai, J. et al. Production of biologically active taxoids by a callus culture of *Taxus cuspidata*. *J. Nat. Prod.* **67**, 58–63 (2004).
- Leung, K.W. & Wong, A.S.-T. Pharmacology of ginsenosides: a literature review. *Chin. Med.* **5**, 20 (2010).
- Dan, M. et al. Metabolite profiling of *Panax notoginseng* using UPLC-ESI-MS. *Phytochemistry* **69**, 2237–2244 (2008).
- Reynolds, L.B. Effects of harvest date on some chemical and physical characteristics of American ginseng (*Panax quinquefolius* L.). *J. Herbs Spices Med. Plants* **6**, 63–69 (1998).
- Kutchan, T. & Dixon, R.A. Physiology and metabolism: Secondary metabolism: nature's chemical reservoir under deconvolution. *Curr. Opin. Plant Biol.* **8**, 227–229 (2005).



ONLINE METHODS

Collection and sterilization of *T. cuspidata* samples. Twig, needle and seed samples were collected from a wild-grown *T. cuspidata* tree. Twig and needle samples were immediately deposited in 0.56 mM ascorbic acid solution. They were stored at 4 °C for 1 month. Then, they were washed in running tap water for 30 min and surface disinfected with 70% ethanol for 1 min, followed by 1% sodium hypochlorite for 20 min for twigs and 15 min for needles and 0.07% NaOCl for 20 min, and rinsed 5 times with sterilized distilled water (dH₂O). Lastly, they were rinsed once with dH₂O containing 150 mg/l citric acid. Seeds were put into 0.01% NaOCl for 24 h with agitation. They were washed in running tap water for 4 h, surface disinfected with 70% ethanol for 1 min and then placed in a 1% NaOCl for 15 min. Then, they were rinsed 5 times with dH₂O.

Isolation of CMCs. For CMCs, cambium, phloem, cortex and epidermal tissue were peeled off from the xylem and the epidermal tissue side was laid on B5 medium³¹ excluding (NH₄)₂SO₄ with 1 mg/l picloram, 30 g/l sucrose and 4 g/l gelrite. After 4 to 7 d, cell division was evident only in cambium and after 15 d, DDCs started to form from the layer that consisted of phloem, cortex and epidermis by dedifferentiation. At 30 d post-culture, there was a visible split between cambium cells and DDCs of the phloem, cortex and epidermis. This separation was obvious because cambium cells uniformly divided resulting in the formation of a flat plate of cells. In contrast, DDCs derived from phloem, cortex and epidermis proliferated in an irregular form, presumably due to the discrepancy between cell division rates. Following the natural separation of cambium from the other cell types, this cell layer was transferred onto different Petri dishes containing B5 medium excluding (NH₄)₂SO₄ with 1 mg/l picloram, 10 g/l sucrose and 4 g/l gelrite. Initial cell inoculum size was 3.0 g (f.c.w.) and subsequently, CMCs were subcultured onto the fresh medium every 2 weeks. Establishment of *P. ginseng* CMCs was as described above except that the isolation medium contained McCown woody plant medium with 2 mg/l IAA, 30 g/l sucrose, 100 mg/l ascorbic acid, 150 mg/l citric acid and 3 g/l gelrite. For lignin visualization, tissues were stained with phloroglucinol-HCl (0.5% (wt/vol) phloroglucinol in 6 N HCl) for 5 min and then observed under a light microscope.

Establishment of cell suspension cultures and natural product production. Initial suspension cultures were established by inoculating a sample of 2.5 g (f.c.w.) cultured cells derived from either cambium, needles or embryos into 125 ml Erlenmeyer flasks containing 25 ml of B5 medium containing 1 mg/l picloram, and 20 g/l sucrose, excluding (NH₄)₂SO₄. The flasks were agitated at 100 r.p.m. and 21 °C in the dark. Subculturing was undertaken at 2-week intervals.

For culturing the cells in 3 liter and 20 liter air-lift bioreactors, the same medium that was used in the initial suspension culture was applied. Diameter, height and pore size of micro-sparger used in the bioreactor was 2 cm, 0.4 cm, 0.2 μm, respectively. Aeration rate was 0.1–0.2 vol/vol/min (v.v.m.) in 3 liter air-lift bioreactor, and 0.08–0.18 v.v.m. in 20 liter air-lift bioreactor. 3.25 g/l (d.c.w.) of CMCs, 3.3 g/l (d.c.w.) of needle-derived DDCs and 3.1 g/l (d.c.w.) of embryo-derived DDCs were inoculated in 3 liter air-lift bioreactor. 3.65 g/l (d.c.w.) of CMCs, 3.64 g/l (d.c.w.) of needle-derived DDCs and 3.41 g/l (d.c.w.) of embryo-derived DDCs were inoculated in 20 liter air-lift bioreactor. Working volume was 80% of total capacity, which is 2.4 liters in 3 liter air-lift bioreactor and 16 liters in 20 liter air-lift bioreactor. Subculturing of CMCs and DDCs was undertaken every 2 weeks in 3 liter and 20 liter air-lift bioreactor with same initial inoculum size and conditioned medium was recycled with the ratio of 25% of working volume. Growth rate was measured in d.c.w. (g/l) after vacuum filtration and drying of the cells in an oven at 70 °C for 24 h. We call these CMCs Ddobyul, meaning ‘another star’ in Korean.

To test the capacity for production of paclitaxel in the flask and 3 liter and 20 liter air-lift bioreactors, cells at 14 d of culturing were transferred to B5 medium excluding KNO₃, and containing 60 g/l fructose and 2 mg/l 1-naphthalene acetic acid (NAA), and elicitors such as 50 mg/l, chitosan and 100 μM methyl-jasmonate, in addition to 0.1 mM of the precursor, phenylalanine.

Me-JA was dissolved in 90% ethanol, chitosan in glacial acetic acid and phenylalanine in distilled water before dilution to the required concentrations. After 10 d, paclitaxel content was analyzed. Taxane and abietane production was

elicited in a similar fashion. Stress-triggered ginsenoside accrual was mediated by reducing air supply from a constant 0.1 v.v.m. into a 3 liter air-lift bioreactor, for 13 d of culture, to 0.1 v.v.m. for a 30 min period twice per day for 3 d.

Establishment of needle and embryo DDC cultures. DDCs were induced from embryos and needles largely as previously described^{32,33}. For induction of needle-derived DDCs, both ends of the needle were cut in 0.3–0.5 cm (length and width) and were laid on B5 medium containing 1 mg/l picloram, 30 g/l sucrose and 4 g/l gelrite, excluding (NH₄)₂SO₄. After 30 d of culturing, DDCs were induced from the cut edges (Fig. 1f). As culture period continued, DDCs formed over the whole explants. Induced DDCs were transferred to B5 medium containing 1 mg/l picloram, 10 g/l sucrose and 4 g/l gelrite, excluding (NH₄)₂SO₄ for growth. Initial inoculum size was 3.0 g (f.c.w.) and DDCs were subcultured to fresh medium every 2 weeks.

For induction of embryo-derived DDCs, both ends of the zygotic embryo were cut and laid on B5 medium containing 1 mg/l 2,4-D, 30 g/l sucrose and 4 g/l gelrite, excluding (NH₄)₂SO₄. After 23 d of culturing, DDCs were induced from the cut edges (Fig. 1g). As culture period continued, DDCs formed over the whole explant. Induced DDCs were transferred to B5 medium containing 1 mg/l picloram, 10 g/l sucrose and 4 g/l gelrite, excluding (NH₄)₂SO₄ for growth. Initial inoculum size was 3.0 g (f.c.w.) and DDCs were subcultured to fresh medium every 2 weeks.

CMC differentiation. The media used to induce CMC differentiation into tracheary elements (TEs) was B5 medium, excluding (NH₄)₂SO₄ with 10 mg/l NAA, 2 mg/l kinetin, 6 mg/l GA₃ and 60 g/l sucrose. TEs were identified by virtue of their bright fluorescence, due to the presence of lignified secondary cell walls. The extent of TE differentiation was determined as the percentage of TEs per total number of cells. This analysis was undertaken in triplicate and in each case 200 cells were counted.

Response of *T. cuspidata* cell suspensions to γ-irradiation and radiomimetic drugs. CMCs and needle-derived DDCs were obtained from suspension cultures obtained from 20 liter air-lift bioreactors. For gamma-irradiation (Co⁶⁰), cells were irradiated at a dose rate of 0.92 Gy/min for 0–400 Gy, which has been modified from a method described previously³⁴. Then, cells were suspension cultured for 24 h in 100 ml flasks at 21 °C, 100 r.p.m. in the dark (volume of cells to liters of medium was 1:10). Suspension cells were treated with Zeocin (200 μg/ml, Invitrogen) at 7 d after subculture, essentially as described previously³⁴. The treated suspension cell culture was incubated in the dark for 24 or 48 h. For cell death determination, cells were treated with 2% Evan's blue for 3 min and washed with sterile water several times, then transferred to a microscope slide covered with a thin cover slip. For each sample, cell death was determined 5 times independently and the average cell death rate was measured by excluding the maximum and minimum number of cell counts. All experiments were undertaken in triplicate.

Determination of *T. cuspidata* transcriptome. RNA was isolated using a Qiagen plant RNA kit following the manufacturer's instructions. cDNA was synthesized by employing a SMART procedure to enrich for full-length sequences³⁵. The resulting cDNA was normalized using kamchatka crab duplex-specific nuclease³⁶, to aid the discovery of rare transcripts. cDNA was sheared using Covaris instruments settings: target size 500 bp, duty cycle 5%, intensity 3, cycles/burst 200 and time 90 s. Library preparation was undertaken using a Roche GS FLX library kit. The concentration and quality of the synthesized library was analyzed using a Agilent bio-analyzer. Titration emulsion PCR using a GS FLX emPCR kit was undertaken to determine the optimum number of beads to load for large-scale sequencing. A Beckman/Coulter Multisizer 3 bead counter was employed to determine the concentration of beads. Two million beads were loaded onto a GS FLX pico titer plate using a Roche 70 × 75 kit.

The sequencing reagents used and washes undertaken followed protocols from the manufacturer. The *T. cuspidata* transcriptome was determined in the GenePool genomics facility at the University of Edinburgh using a Roche 454 GS FLX instrument in titanium mode, which uses massively parallel pyrosequencing technology^{37,38}. A total of 860,800 reads were achieved of 351 bp average length, which generated 301 MB of sequence. These data were

assembled into isotigs by employing Newbler 2.3. BLAST was used to search for similar sequences within available sequence databases. Annot8r was employed to predict GO terms for each isotig³⁹.

Digital gene expression tag profiling. The analysis of global gene expression in *T. cuspidata* cell suspension cultures was carried out by digital gene expression tag profiling, using an improved method based on previously described technology⁴⁰. Potentially contaminating DNA was removed from RNA samples using Ambion turbo DNase treatment. NlaIII library preparation was accomplished by following the manufacturer's standard protocol. Fifteen PCR cycles were used for amplification. We used 1–10 µg of a given library for sequencing from each sample. Sequencing was carried out in the GenePool genomics facility at the University of Edinburgh using a Genome Analyser (GA) II_x Illumina Solexa sequencing machine. Three replicates each of both cell lines (CMC/DDC) were sequenced following the manufacturer's protocol. Subsequently, reads were aligned to the *T. cuspidata* reference genome using MAQ v. 6.0.8. and uniquely aligned reads to the previously assembled *T. cuspidata* transcriptome were counted.

Statistical analysis. Statistical analysis was performed in R using the edgeR Bioconductor library^{40,41}. We sought to reduce problems created by varying library sizes and noise for genes not highly expressed, by stabilizing read counts through adding a small constant. Therefore we first rescaled the read counts in each library by dividing by the sum of all read counts in the upper quartile of expression values⁴² and afterwards added a constant factor C (C = 10) to each count. This transformation alters the signal in such a way that differences between groups for contigs with low expression are less likely to be considered differentially expressed, while leaving high transcript counts largely untouched. Briefly, edgeR uses an overdispersed Poisson distribution to model read count data, where the degree of overdispersion is moderated using an empirical Bayes procedure. Differential expression is assessed using a modified version of Fisher's exact test. We ran edgeR according to the steps outlined in the library's tutorial (using parameter settings prior. $n = 10$, grid.length = 500). P-values were adjusted for the false discovery rate and we deemed a threshold of false discovery rate (FDR) ≤ 0.05 to be appropriate to detect differentially expressed contigs ($n = 1,229$).

In the latter analysis, we decided to first focus on only those differentially expressed contigs, that showed a considerably large change (that is, the minimum difference between any replicates in both groups, DDC and CMC, was at least ten transcripts per million) and for which the direction of change was consistent between all replicates (that is, all replicates are either higher or all replicates are lower in one group than in the other). We considered these filtered contigs ($n = 563$) the most interesting candidates for immediate study and held out the rest for further follow-up studies.

Gene expression analysis. The determination of gene expression levels were carried out by either RT-PCR or qRT-PCR as previously described⁴³. The primer sequences employed are listed below:

Primer sequences for qRT-PCR.

Ct01805-F: CTTGGCAAGGATCCAGTTTAG

Ct01805-R: AGACCAAGCCCAGGGTCTTC

Ct10710-F: TTCTTCGGCTGTCTCAGTGATG

Ct10710-R: CCGATAGAAGCTTGCAGGAA

Primer sequences for RT-PCR.

Ct27072-F: CACTTGGAGTTCGTCGTTGA

Ct27072-R: CACTGTGCACACTACCCAAA

Ct36802-F: GAGCCGTTGCATGGTACACT

Ct36802-R: TAACCGTGGTGTCAAATCA

Ct18649-F: CCTGACAACAGCGTCTCTGA

Ct18649-R: AAACCACAGTACCCACAGC

Ct33753-F: GTTAGACCCTTACCCTGCA

Ct33753-R: CTGCAAAGCTGAGAGTGGAAATG

Ct30863-F: GCAACGTCTGAAACGCAGTA

Ct30863-R: AGAGTTGCCAACAGCAAAGG

Ct34959-F: ACTCGATAGACCGACAAGG

Ct34959-R: CAGCTGATCGTCCAGCTATG

Ct01720-F: CTCCTCTCAACGAGGAAAA

Ct01720-R: GTTTTCCCAGAAGGGAATC

Ct09814-F: TTTGAGGCATGTGGGTTTAA

Ct09814-R: TGTCATCTGTTGCATTGGA

Ct07968-F: CGACAACATTCTTGCATTGA

Ct07968-R: AACCGTTGCAGGGAACCTAC

Ct03409-F: ATGTTCCAAAAATGGGAGGA

Ct03409-R: GCTTGGAAAAGACCTGAAGGA

Ct04884-F: AGTGAATGTAAGCCCCATGA

Ct04884-R: TTTGGCATCTTCTGGATGA

Ct07286-F: GTCCATCCATTGTCCATAGAAA

Ct07286-R: TGGCAACATTGGTAAAGATATTCA

Perfusion culture. Perfusion culture was initiated in a similar fashion to that described for the bioreactors. On day 14, cultures were elicited with 50 mg/l chitosan, 0.1 mM phenylalanine and 100 µM methyl jasmonate. After elicitation, the spent medium was removed aseptically and replaced with an equal volume of fresh B5 medium excluding KNO₃ with 60 g/l fructose and 2 mg/l 1-naphthalene acetic acid (NAA) and elicitors of 50 mg/l chitosan, 0.1 mM phenylalanine and 100 µM methyl-jasmonate every 5 d. After 45 d of extended culture, intracellular and extracellular paclitaxel levels were analyzed.

Analysis of taxanes (paclitaxel, baccatin III, 10-deacetyl baccatin III) content.

After their separation from the production medium, 0.2 g of cells were weighed, soaked in 4 ml of methanol (Sigma)/dichloromethane (Sigma) (1:1 vol/vol) and sonicated (Branson) for 1 h. The methanol/dichloromethane extract (4 ml) was filtered and concentrated *in vacuo* and subsequently redissolved in 4 ml of dichloromethane and partitioned with 2 ml of water. The latter step was repeated three times and only the dichloromethane fraction was collected. This fraction was concentrated, then redissolved in 1 ml of methanol and centrifuged at 8,000g for 3 min before HPLC analysis. For determining the extracellular paclitaxel concentration, production medium (5 ml) was extracted 3 times with the same volume of dichloromethane. The combined dichloromethane fraction was subsequently concentrated and then redissolved in 0.5 ml methanol. HPLC (nanospace SI-2, Shiseido) with a C18 column (Capcell pak C18 MGII column, 5 µm, 3.0 mm × 250 mm, Shiseido) was used for the analysis. Column temperature was 40 °C and the mobile phase was a mixture of water and acetonitrile (Burdick & Jackson) (1:1 isocratic) at a flow rate of 0.5 ml/min. A UV-VIS detector monitored at 227 nm and the sample injection volume was 10 µl. Authentic paclitaxel, baccatin III, 10-deacetyl baccatin III standard was purchased from Sigma.

Analysis of abietanes (taxamairin A and taxamairin C) content.

After their separation from the production medium, 20 mg of lyophilized cells were weighed, soaked in 4 ml of methanol (Sigma)/dichloromethane (Sigma) (1:1 vol/vol) and sonicated (Branson) for 1 h. The methanol/dichloromethane extract (4 ml) was filtered and concentrated *in vacuo* and subsequently redissolved in 4 ml of dichloromethane and partitioned with 2 ml of water. The latter step was repeated three times and only the dichloromethane fraction was collected. This fraction was concentrated, then redissolved in 1 ml of methanol and centrifuged at 8,000g for 3 min. Then it was filtered through 0.2 µm filter for UPLC analysis. UPLC (Waters) with a C18 column (BEH C18 1.7 µm, 2.1 × 100 mm Waters) was used for the analysis. Column temperature was 40 °C and the mobile phase was a mixture of water and acetonitrile (Burdick & Jackson) flow rate of 0.4 ml/min. Water (solvent A) and acetonitrile (solvent B) as mobile phase with a linear gradient was used: (1 min: 0% B, 13 min: 100% B, 15 min: 100% B, 16.2 min: 0% B, 17 min: 0% B). A UV-VIS detector monitored at 210 nm and the sample injection volume was 2 µl. Authentic taxamairin A and taxamairin C standard were isolated at Unhwa.

Analysis of ginsenosides (ginsenoside F2, gypenoside XVII) content.

Compounds of *Panax ginseng* CMCs were analyzed through HPLC-ELSD (Younglin) and two major peaks were isolated. The two compounds isolated were identified as ginsenoside F2 and gypenoside XVII through LC-MS (Agilent), ¹H NMR, ¹³C NMR and 2D NMR (Varian). For quantification of ginsenoside F2 and gypenoside XVII in *Panax ginseng* CMCs, cultured cells

were separated from the medium and were lyophilized. 100 mg of lyophilized cells were put into 2 ml of methanol (Sigma), vortexed for 5 min, and were extracted for 1 h. Cells were centrifuged at 8,000g for 3 min. After concentration of the supernatant, it was dissolved in 200 μ l of methanol and filtered through 0.2 μ m filter for UPLC analysis. UPLC with a C18 column (BEH C18 1.7 μ m, 2.1 \times 100 mm Waters) was used for the analysis. Column temperature was 40 $^{\circ}$ C and the mobile phase was a mixture of water and acetonitrile (Burdick & Jackson), flow rate of 0.4 ml/min. Water (solvent A) and acetonitrile (solvent B) as mobile phase with a linear gradient was used: (0 min: 0% B, 9 min: 100% B, 11 min: 100% B, 11.2 min: 0% B, 12 min: 0% B). A UV-VIS detector monitored at 203 nm and the sample injection volume was 2 μ l. Standard of gypenoside XVII were isolated by Unhwa. Ginsenoside F2 was purchased from LKT Laboratories.

Microscopy. Light microscopy was undertaken using a model BX41, Olympus. A polarizer for transmitted light, model U-POT, Olympus, was used for TE images. TEs were identified by virtue of their bright fluorescence, due to the presence of lignified secondary cell walls.

Vacuole experimentation was undertaken based on modifications of the methods described previously^{44,45}. Briefly, CMCs, needle- and embryo-derived DDCs were stained with 0.01% (wt/vol) neutral red (SIGMA-ALDRICH) for 3 min. Then, cells were washed with 0.1 M phosphate buffer (pH 7.2) and were observed with an optical microscope (BX41 Olympus) using the same buffer.

LC-MS. Analysis was undertaken using an HP 1100 Series liquid chromatography/HP 1100 Series mass selective detector (Agilent Technologies). Samples (2 μ l) were separated on a PerfectSil Target ODS-3 (4.6 mm \times 150 mm \times 3 μ m) using water (10 mM ammonium acetate): acetonitrile which was isocratic: 50% acetonitrile for 60 min, at 0.4 ml/min flow rate. Mass detection of paclitaxel was by electrospray ionization (ESI) in the positive ion mode. The drying gas was N₂ at 10 l/min, 350 $^{\circ}$ C, 30 p.s.i. The vaporizer was set to

300 $^{\circ}$ C, capillary to 4,000 V. Identification of paclitaxel was accomplished by comparison of retention times and mass with authentic standards.

31. Gamborg, O.L., Miller, R.A. & Ojima, K. Nutrient requirements of suspension cultures of soybean root cells. *Exp. Cell Res.* **50**, 151–158 (1968).
32. Zang, X., Mei, X.-G., Zhang, C.-H., Lu, C.T. & Ke, T. Improved paclitaxel accumulation in cell suspension cultures of *Taxus chinensis* by brassinolide. *Biotechnol. Lett.* **23**, 1047–1049 (2001).
33. Yukimune, Y., Tabata, H., Higashi, Y. & Hara, Y. Methyl jasmonate-induced overproduction of paclitaxel and baccatin III in *Taxus* cell suspension cultures. *Nat. Biotechnol.* **14**, 1129–1132 (1996).
34. Fulcher, N. & Sablowski, R. Hypersensitivity to DNA damage in plant stem cell niches. *Proc. Natl. Acad. Sci. USA* **106**, 20984–20988 (2009).
35. Zhu, Y.Y., Machleder, E.M., Chenchik, A., Li, R. & Siebert, P.D. Reverse transcriptase template switching: A SMART™ approach for full-length cDNA library construction. *BioTech.* **30**, 892–897 (2001).
36. Zhulidov, P.A. *et al.* Simple cDNA normalization using Kamchatka crab duplex-specific nuclease. *Nucleic Acids Res.* **32**, e37 (2004).
37. Margulies, M. *et al.* Genome sequencing in open microfabricated high-density picoliter reactors. *Nature* **437**, 376–380 (2005).
38. Brenner, S. *et al.* Gene expression analysis by massively parallel signature sequencing (MPSS) on microbead arrays. *Nat. Biotechnol.* **18**, 630–634 (2000).
39. Schmid, R. & Blaxter, M.L. annot8r: GO, EC and KEGG annotation of EST datasets. *BMC Bioinformatics* **9**, 180 (2008).
40. Robinson, M.D., McCarthy, D.J. & Smyth, G.K. edgeR: a Bioconductor package for differential expression analysis of digital gene expression data. *Bioinformatics* **26**, 139–140 (2010).
41. Gentleman, R.C. *et al.* Bioconductor: open software development for computational biology and bioinformatics. *Genome Biol.* **5**, R80 (2004).
42. Bullard, J.H., Purdom, E., Hansen, K.D. & Dudoit, S. Evaluation of statistical methods for normalization and differential expression in mRNA-Seq experiments. *BMC Bioinformatics* **11**, 94 (2010).
43. Nolan, T., Hands, R.E. & Bustin, S.A. Quantification of mRNA using real-time RT-PCR. *Nat. Protoc.* **1**, 1559–1582 (2006).
44. Kataoka, T. *et al.* Vacuolar sulfate transporters are essential determinants controlling internal distribution of sulfate in *Arabidopsis*. *Plant Cell* **16**, 2693–2704 (2004).
45. Lee, Y. *et al.* The *Arabidopsis* phosphatidylinositol 3-kinase is important for pollen development 1. *Plant Physiol.* **147**, 1886–1897 (2008).